MOLECULAR AND CELLULAR BIOLOGY, June 2006, p. 4664–4674 Vol. 26, No. 12
0270-7306/06/$08.00+0 doi:10.1128/MCB.02253-05

Concerted Functions of Gab1 and Shp2 in Liver Regeneration and Hepatoprotection

Emilie A. Bard-Chapeau,[1] Jing Yuan,[1] Nathalie Droin,[3] Shinong Long,[1] Eric E. Zhang,[1,2] Thanh V. Nguyen,[1] and Gen-Sheng Feng[1,2]*

Programs in Signal Transduction and Stem Cells and Regeneration, The Burnham Institute for Medical Research, 10901 N. Torrey Pines Rd., La Jolla, California 92037[1]; Department of Pathology, University of California at San Diego, La Jolla, California 92093[2]; and Division of Cellular Immunology, La Jolla Institute for Allergy and Immunology, San Diego, California 92121[3]

Received 22 November 2005/Returned for modification 12 January 2006/Accepted 5 April 2006

Liver regeneration is a rapid and concerted response to injury, in which growth factor-generated intracellular signals result in activation of transcription factors, DNA synthesis, and hepatocyte proliferation. However, the link between cytoplasmic signals resulting in proliferative response to liver injury remains to be elucidated. We show here that association of Gab1 adaptor protein and Shp2 tyrosine phosphatase is a critical event at the early phase of liver regeneration. Partial hepatectomy (PH) rapidly and transiently induced assembly of a complex comprising Shp2 and tyrosine-phosphorylated Gab1 in wild-type hepatocytes. Consistently, liver-specific Shp2 knockout (LSKO) and liver-specific Gab1 knockout (LGKO) mice displayed very similar phenotypes of defective liver regeneration triggered by PH, including blunted extracellular signal-regulated kinase 1/2 (Erk1/2) activation, decreased expression of immediate-early genes, and reduced levels of cyclins A, E, and B1, as well as suppression of hepatocyte proliferation. In contrast, the Akt and interleukin-6/Stat3 pathways were up-regulated posthepatectomy in LSKO and LGKO mice, accompanied by improved hepatoprotection. Collectively, this study establishes the physiological significance of the Gab1/Shp2 link in promoting mitogenic signaling through the Erk pathway in mammalian liver regeneration.

Liver regeneration, a unique capacity conserved in humans, possibly evolved to protect wild animals from catastrophic damage to the liver by toxic foods. This remarkable growth property has fascinated biologists for nearly a century, and the most frequently used experimental model to analyze liver regeneration is the partial hepatectomy (PH), established by Higgins and Anderson in 1931, in which two-thirds of a rat liver was removed (9, 16, 30). Hepatocytes are normally in a quiescent state, and following PH, more than 95% of the mature and quiescent cells in the remnant liver reenter the cell cycle and rapidly divide for one or more rounds, resulting in restoration of the hepatic mass within 7 to 10 days.

Immediately following PH, the concentrations of a number of cytokines, growth factors, and hormones rise dramatically in the plasma or locally in the liver (10). In particular, hepatocyte growth factor/scatter factor (HGF/SF), epidermal growth factor (EGF), transforming growth factor α, tumor necrosis factor alpha (TNF-α), insulin, and interleukin-6 (IL-6) play pivotal roles in mitogenic and antiapoptotic responses. Fausto and colleagues have proposed that in the initial stage of liver regeneration, hepatocytes enter a state of replicative competence, or "priming," and then become fully responsive to proliferative signals (10). The immediate-early genes, such as c-*Fos*, c-*Jun*, and c-*Myc*, are among the first group of genes induced by PH (9). Haber et al. have identified as many as 70 genes that are involved in liver regeneration (14). A recent microarray analysis identified a variety of genes induced in the early phase of liver regeneration (43).

Several groups have reported PH-triggered activation of the extracellular signal-regulated kinase (Erk) (9, 19, 24, 46). Liver-specific deletion of c-Met resulted in suppression of the Erk pathway and impaired liver regeneration (6, 19). Activation of Stat3 appears to be required for IL-6 induction of immediate-early genes posthepatectomy (7). Liver-specific inactivation of the *Stat3* gene led to impaired DNA synthesis in hepatocytes following PH (25). Activation of IL-6/Stat3 signaling has also been reported to protect the liver parenchyma from stress and infectious injury (5, 22, 47, 48, 56).

There is a gap in our knowledge about the molecular link that couples cytoplasmic signals initiated by growth factors/cytokines. Gab1 (Grb2-associated binder 1) is an adaptor/scaffold protein that contains a pleckstrin homology domain at the N terminus, proline-rich motifs for association with Src homology 3 (SH3)-containing molecules, and a dozen putative tyrosyl residues that may couple with SH2-containing proteins (13, 17, 26). In response to stimulation by growth factors in vitro, Gab1 undergoes tyrosine phosphorylation and association with Shc, CrkL, phospholipase Cγ (PLC-γ), p85, and Shp2, and Gab1 has been implicated in promotion of the Erk pathway (13, 26). Targeted deletion of Gab1 in mice resulted in embryonic lethality in homozygotes, with defects in placenta, liver growth and development, and impaired Erk1/2 activation, a phenotype similar to HGF or c-Met knockout animals (4, 20, 27, 37, 40, 50).

Shp2 is a ubiquitously expressed protein tyrosine phosphatase with two SH2 domains that is involved in signaling events proximal to receptor tyrosine kinases or cytokine recep-

* Corresponding author. Mailing address: The Burnham Institute for Medical Research, 10901 N. Torrey Pines Rd., La Jolla, CA 92037. Phone: (858) 713-6265. Fax: (858) 713-6274. E-mail: gfeng@burnham.org.

tors (23, 32). Homozygous disruption of the *Shp2* gene leads to embryonic lethality in mice and reveals crucial roles in cell differentiation and developmental processes, such as hematopoiesis and morphogenic movements of gastrulation (36, 38, 39). Physical association of Shp2 with various adaptor/scaffold proteins has been observed in several cell types (23, 32, 35). In particular, Shp2 has been shown to bind Gab1 by recognizing two phosphotyrosine (p-Tyr) residues (p-Tyr^{627} and p-Tyr^{659}) at the C-terminal tail of Gab1 (8), and the Gab1/Shp2 interaction has been implicated in activation of Erk1/2 in vitro (13, 26).

It remains to be determined whether the association of Gab1 with Shp2 plays a nonredundant role in mitogenic signaling in vivo. Apparently, Gab1 may couple to a variety of SH3- and SH2-containing molecules, and Shp2 can also associate with various adaptor/scaffold proteins, such as Gab2, Gab3, and insulin receptor substrate 1 (IRS1) to IRS4, in cytoplasmic signaling (23, 32). To determine the functions of Gab1 and Shp2 individually and also to define the physiological significance of the Gab1/Shp2 association in proliferative signaling in vivo, we created liver-specific Shp2 knockout (LSKO) and liver-specific Gab1 knockout (LGKO) mice and examined PH-triggered liver regeneration. Despite the existence of multiple partners for either Gab1 or Shp2, we demonstrate that the Gab1/Shp2 interaction plays an indispensable role in signal relay for hepatocyte proliferation triggered by PH. This study thus identifies the Gab1/Shp2 partnership as a missing link in intracellular signaling pathways functioning in liver regeneration.

MATERIALS AND METHODS

Mice. All animals were housed in a virus-free, temperature/light (12-hour light/dark cycle)-controlled animal facility. Mice were permitted ad libitum access to water and standard chow food. The institutional animal committee approved all protocols for animal use and euthanasia. LGKO mice (C57BL/6 background) were described previously (2), and generation of *Shp2*^{flox} mice was reported elsewhere (53). *Shp2*$^{flox/flox}$ mice were mated with *Albumin-Cre* transgenic mice [C57BL/6-TgN (Alb-cre)21Mgn] obtained from the Jackson Laboratory (34) to obtain LSKO mice (*Shp2*$^{flox/flox}$*:Alb-Cre*/+). Both *Shp2*$^{flox/flox}$ and *Gab1*$^{flox/flox}$ littermates were used as controls, and the experiments were done on 8- to 10 week-old male mice. Genotyping was done by PCR analysis on tail genomic DNA (2, 53). For partial hepatectomy, two-thirds of the liver mass was removed. Mice were anesthetized with Avertin (0.015 ml/g of body weight) and subjected to a resection of left lateral, left median, and right median lobes; the gallbladder was also carefully removed. Lobes were ligated together with silk suture and excised through a 1-cm longitudinal abdominal incision, which was closed in two layers. At the indicated time points, animals were sacrificed and their remnant lobes were harvested. Unlike the liver-specific c-Met knockout mice (6, 19), both LGKO and LSKO mutant animals survived the surgical procedure. Hepatocytes were isolated by collagenase digestion of liver pieces (42). Cells were plated in Dulbecco modified Eagle medium with 10% fetal bovine serum for 24 h, and the total proteins were extracted by incubation with protein lysis buffer.

BrdU labeling and immunohistochemistry. Two hours before harvesting the remnant liver, animals were injected intraperitoneally with 5-bromo-2′-deoxyuridine (BrdU), 50 mg/g of body weight. Mice were sacrificed at the indicated time points, and the three withdrawn lobes were quickly frozen in OCT (optimal cutting temperature) compound (Tissue-Tek), cryosectioned (5-μm thickness) and prepared for immunostaining. BrdU labeling and detection kit I (Roche) was used and Vectashield mounting medium with 4′,6′-diamidino-2-phenylindole (DAPI) (Vector) was used to stain nuclei. The number of BrdU-positive hepatocytes was calculated by randomly counting the BrdU-stained nuclei per 100 DAPI-labeled nuclei in a total of at least 3,000 hepatocytes (1,000 hepatocytes per lobe). Statistical analysis was performed using a two-tailed unpaired *t* test.

In vivo stimulation of the liver with HGF, EGF, and IL-6. Under anesthesia with Avertin (0.015 ml/g body weight), the abdominal cavity of mice that had gone 16 h without food was opened widely and the portal vein exposed. Either 50 μl saline or 50 μl saline containing 3.3 μg human HGF, 5 μg murine IL-6, or 5 μg murine EGF (Peprotech, Inc.) was injected into the portal vein, and the livers were harvested 5 min later and quickly frozen in liquid nitrogen.

Serological analyses. Venous blood was collected by bleeding of the retro-orbital sinus, prior to sacrifice. Serum IL-6 levels were determined using the IL-6 mouse Biotrak enzyme-linked immunosorbent assay system (Amersham Biosciences). Alanine aminotransferase (ALT) and aspartate aminotransferase (AST) levels were measured by the Animal Care Program, Diagnostic Laboratory, University of California at San Diego. Statistical analysis was performed using a two-tailed unpaired *t* test.

Biochemical analyses. Frozen tissue samples were homogenized in a Dounce apparatus in protein lysis buffer (44), tissue lysates were clarified by centrifugation at 37,000 × *g* for 1 h at 4°C, and protein concentration was determined using a Bio-Rad kit. Immunoprecipitation with 1.5 mg of total proteins was done with protein A/G plus agarose (Santa Cruz), and the immunoprecipitates were washed three times with cold HNTG buffer (41). Samples of immunoprecipitates or lysates were subjected to immunoblotting with appropriate antibodies and detected by an ECL kit (Amersham). Antibodies against Shp2 or Gab1 were produced in our laboratory (41, 44). Antibodies to phospho-Erk1/2 (p-Erk1/2), p-Tyr^{705}Stat3, Stat3, p-Akt, Akt, phosphorylated glycogen synthase kinase 3 (p-GSK3), GSK3, phosphorylated murine double mutant 2 (p-MDM2), p-Bad, Bad, phosphorylated p38 (p-p38), p38, p-Met, p-EGFR, EGF receptor (EGFR), and the p85 subunit of phosphatidylinositol 3-kinase (PI3K) were from Cell Signaling. Antibodies to Erk2, Jun N-terminal protein kinase 1/2 (Jnk1/2), RasGAP, MDM2, Grb2, PLC-γ, and pan-Fos were obtained from Santa Cruz; antibodies against p-Jnk1/2 and tubulin were from Promega; and antiphosphotyrosine (anti-PY) and anti-Met antibodies were from Upstate Biotechnology, Inc. Cyclin A, E, B1, and D antibodies were kindly provided by W. Jiang at The Burnham Institute. When needed, films were scanned, and signals were quantified using ImageQuant software. Statistical analysis was performed using a two-tailed unpaired *t* test.

Isolation of cytoplasmic and plasma membrane-enriched fractions. Frozen tissue samples immersed in hypotonic buffer (10 mM Tris-HCl, pH 7.5) were sliced into small pieces before being homogenized in a Dounce homogenizer using the large-clearance piston. After centrifugation at 2,000 × *g* for 15 min to remove cell nuclei and unbroken cells, the lysates were centrifuged at 100,000 × *g* for 30 min to isolate the membrane fraction. The supernatants were kept as cytoplasmic fractions, and the pellets were washed three times in cold phosphate-buffered saline before being dissolved in radioimmunoprecipitation assay buffer. The new lysates were shaken for 30 min at 4°C and centrifuged at 20,000 × *g* for 10 min, and the supernatant was collected as plasma membrane-enriched fractions.

Electrophoretic gel mobility shift assay. Nuclear proteins were extracted from fresh liver using a nuclear extract kit (Active Motif), according to the manufacturer's instructions. An oligonucleotide carrying consensus Stat3 binding motif (5′-GATCCTTCTGGGAATTCCTAGATC) was purchased from Santa Cruz, 5′ end labeled, and purified using Microspin G-50 columns (Amersham). DNA-protein binding reaction and gel electrophoresis were done following standard procedures. The supershift was done with 1 μl of Stat3 antibody from Cell Signaling.

Real-time reverse transcription-PCR (RT-PCR). Total RNA was isolated from frozen pieces of liver using RNA Stat-60 reagent (Tel-Test) according to the manufacturer's instructions. Three mice per group were assessed at 0, 1, 4, and 8 h postsurgery. RNA was reverse transcribed by Moloney murine leukemia virus reverse transcriptase (Gibco BRL) with random hexamers (Gibco BRL). For c-*Fos* gene expression, primers were located in separate exons in genomic DNA. Mouse-specific forward and reverse primers, respectively, were as follows: c-*Fos*, 5′-CGGGTTTCAACGCCGAC-3′ and 5′-TGGCACTAGAGACGGACAGATC-3′; c-*Jun*, 5′-CGATGCCCTCAACGCC-3′ and 5′-CTTAGGGTTACTGTAGCCGTAGGC-3′; c-*Myc*, 5′-ATGTTGCGGTCGCTACGTC-3′ and 5′-AGAAGTTGCCACCGCCG-3′; CCAAT enhancer binding protein β (*C/EBP*β), 5′-CACAAGGTGCTGGAGCTGAC-3′ and 5′-AACAAGTTCCGCAGGGTGC-3′; *HGF*, 5′-ATCATTGGTAAAGGAGGCAGCTA-3′ and 5′-AATTCCAAGGCTGGCATTTG-3′; *EGF*, 5′-CCTTCCTGCTGGTGTTTTTAAAG-3′ and 5′-GAGGACCTGGCTGACAGTTCC-3′; *Stat3*, 5′-CACCAACGACCTGCAGCA-3′ and 5′-TGCATCAATGAATCTAAAGTGCG-3′; *IL-6*, 5′-CTGCAAGAGACTTCCATCCAGTT-3′ and 5′-GAAGTAGGGAAGGCCGTGG-3′; *TNF*-α, 5′-ACAGAAAGCATGATCCGCG-3′ and 5′-GCCCCCCATCTTTTGGG-3′; *hemopexin*, 5′-TAGGACAGCAGTGGCGCTA-3′ and 5′-GGCAACAGCCAGGGACC-3′; *Bcl-xl*, 5′-GAATGGAGCCACTGGCCA-3′ and 5′-GCTGCCATGGGAATCACCT-3′; *cyclophilin*, 5′-GGCCGATGACGAGCCC-3′ and 5′-TGTCTTTGGAACTTTGTCTGCAA-3′; and *L32*, 5′-GAAACTG

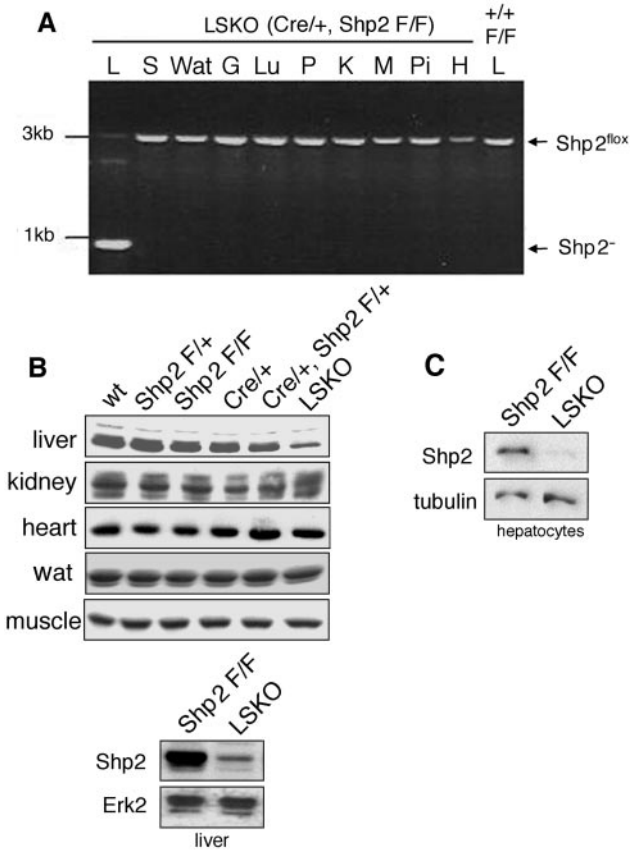

FIG. 1. Selective deletion of *Shp2* in the hepatocytes of LSKO mice. (A) Genotyping of mice by PCR. Genomic DNA was extracted from liver (L), spleen (S), white adipose tissue (Wat), gut (G), lung (Lu), pancreas (P), kidney (K), skeletal muscle (M), pituitary gland (Pi), and hypothalamus (H) of an LSKO mouse (*Cre*/+ *Shp2*$^{flox/flox}$ [Shp2 F/F]) and a *Shp2*$^{flox/flox}$ mouse (+/+ F/F). The *Shp2*^{flox} allele produced a 3-kb fragment, and the *Shp2*$^{-}$ allele gave rise to a 1-kb fragment. Deletion of *Shp2* exon 4 was detected only in the livers of LSKO mice. (B) (Top) Immunoblot analysis of Shp2 protein expression in liver, kidney, heart, white adipose tissue (wat), and skeletal muscle isolated from mice of different genotypes (wt, wild type). (Bottom) Immunoblotting of Shp2 in liver lysates was done with anti-Erk2 blot as a loading control. Shp2 protein content was dramatically reduced in the liver lysate of LSKO mice. (C) Immunoblot analysis of Shp2 in hepatocytes isolated from control or LSKO mice, with tubulin used as a loading control.

GCGGAAACCCA-3′ and 5′-GGATCTGGCCCTTGAACCTT-3′. Real-time PCR was performed with i*Taq* DNA polymerase in a PE Biosystems 5700 thermocycler using the SYBR green detection protocol outlined by the manufacturer. Each gene of interest was normalized against both cyclophilin and L32, allowing comparison of mRNA levels.

RESULTS

Generation of liver-specific Shp2 or Gab1 knockout mice. We created a conditional *Shp2* knockout (*Shp2*^{flox} or *Shp2*^{F}) allele in mice in which two *loxP* sites were inserted into introns that flank exon 4 of *Shp2* (53). *Shp2*$^{flox/flox}$ mice were intercrossed with an *Albumin-cre* (*Alb-Cre*/+) transgenic mouse line (29, 34) to generate LSKO mice (*Shp2*$^{flox/flox}$*:Alb-Cre*/+). PCR analysis showed efficient deletion of the *loxP*-flanking sequence in the liver, but not in other organs or tissue (Fig. 1A). Immunoblot analysis of liver lysates revealed a decrease in Shp2 protein content by 78% in LSKO liver ($n = 5$), with no changes in other tissues/organs of LSKO mice or in the livers of control mice (Fig. 1B). However, immunoblot analysis of hepatocyte lysates derived from LSKO mice demonstrated a nearly complete ablation of Shp2 (Fig. 1C). As previously described (29, 34), *Albumin-Cre* expression started 1 week after birth, and therefore, deletion of Shp2 did not affect liver development. LSKO mice were born with the expected Mendelian frequency and were morphologically indistinguishable from their *Shp2*$^{flox/flox}$ or *Shp2*$^{flox/+}$*:Cre*/+ littermates. In this study, most experiments were conducted as a comparative analysis between control (*Shp2*$^{flox/flox}$*:*+/+) and LSKO (*Shp2*$^{flox/flox}$*:Cre*/+) mice.

In previous studies, we generated a conditional *Gab1* knockout (*Gab1*^{flox}) allele and LGKO animals (*Gab1*$^{flox/flox}$*:Alb-Cre*/+) (2). LGKO mice were healthy and displayed improved glucose tolerance and enhanced hepatic insulin activity relative to wild-type animals (2).

LSKO and LGKO mice display very similar hepatocyte proliferation defects in liver regeneration. We performed a two-third partial hepatectomy followed by a BrdU incorporation assay to count the number of hepatocytes in S phase at several time points posthepatectomy (Fig. 2A and B). BrdU staining was observed at very low levels in liver sections of control and mutant animals before surgery, supporting the notion that hepatocytes are normally in the quiescent G_0 stage. The peak of DNA synthesis occurred 40 h after surgery in control and mutant mice. However, although the kinetics of DNA synthesis was conserved, the maximal levels were decreased by 61.3% and 46.6% in LGKO and LSKO animals, respectively, 40 h posthepatectomy (Fig. 2A and B). Statistically significant differences in DNA synthesis were observed at 36, 40, 44, 48, and 68 h after surgery between control and LSKO mice and at 40, 44, 48, and 68 h between control and LGKO animals. No significant change of mortality or morbidity was observed in either LGKO or LSKO mice after surgery compared to the control animals. In assessing the ratios of the liver mass per body weight at different time points after surgery, we found no difference between control and knockout mice at 24 and 48 h, but the liver mass was lower in LSKO/LGKO mice than in the controls 72 h posthepatectomy (Fig. 2C).

Previous studies correlated hepatocyte cell cycle progression with cyclin expression (3), and thus, we examined the protein levels of cyclins A, B1, E, and D1 at 28, 36, 44, and 68 h posthepatectomy (Fig. 2D). Consistent with the DNA synthesis peak at 40 h, maximal induction of cyclins A, E, and B1 occurred 36 and 44 h after surgery in control liver. Correlated with the reduced mitotic index, expression levels of cyclins A, E, and B1 were markedly reduced in both Shp2- and Gab1-deficient liver lysates, but cyclin D1 expression was normal in the two mutants (Fig. 2D). Similarly reduced levels of cyclins A, E, and B1 but normal expression of cyclin D1 was observed in mice deficient for C/EBPβ or IGFBP-1 (insulin-like growth factor binding protein 1) (12, 24).

Assembly of a signalosome containing Gab1 and Shp2 is critical for PH-initiated hepatocyte proliferation. The similar impaired proliferation phenotype between Shp2- and Gab1-deficient hepatocytes prompted us to investigate the functional interaction of these two molecules in regenerating livers. Liver

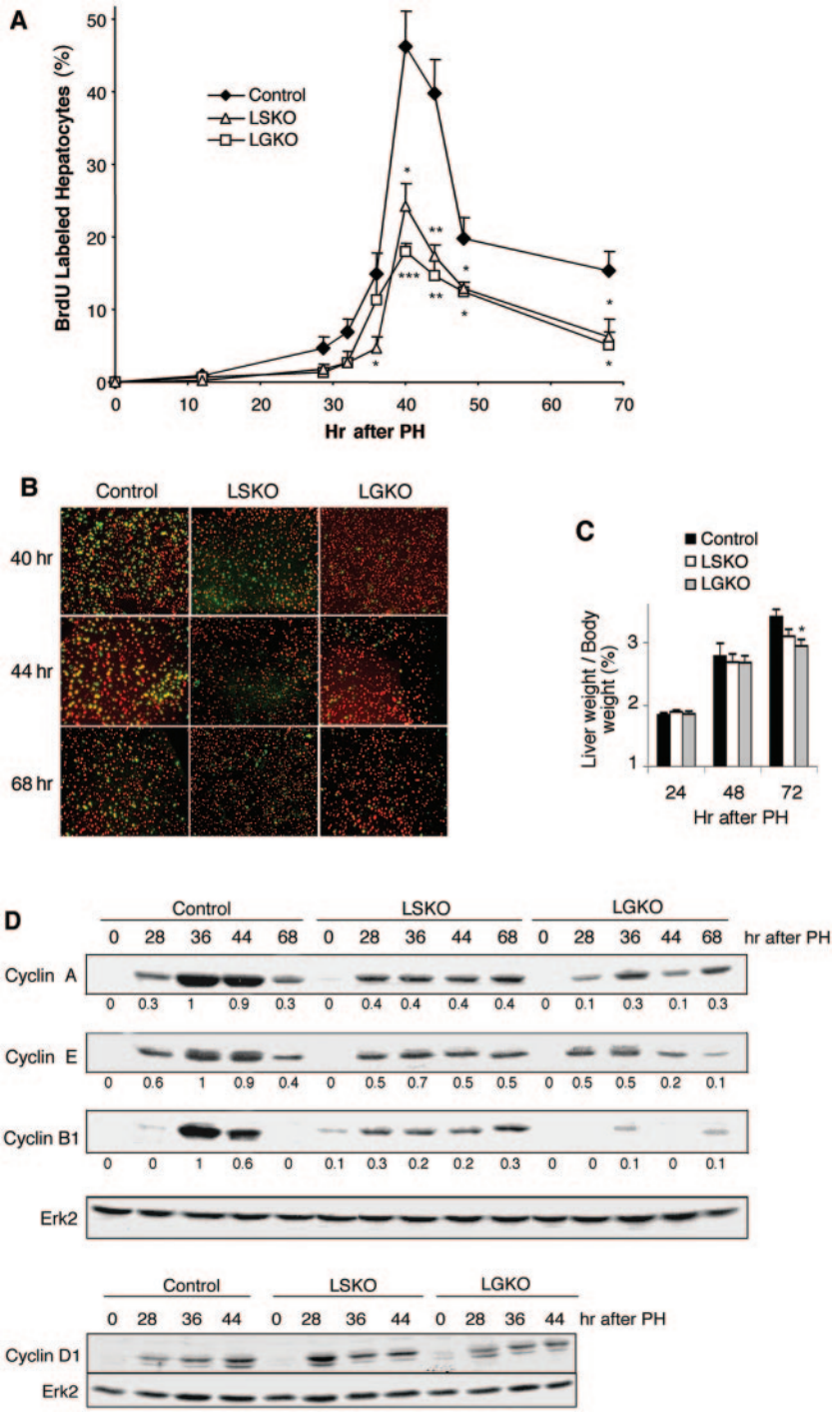

FIG. 2. Reduced hepatocyte proliferation in the livers of LSKO and LGKO mice posthepatectomy. (A) Quantification of BrdU labeling. Control (*Shp2*$^{flox/flox}$ or *Gab1*$^{flox/flox}$), LSKO, and LGKO mice were subjected to partial hepatectomy and were injected with BrdU 2 h before harvest. Animals were sacrificed at the indicated time points, and the number of BrdU-positive hepatocytes was quantified. Values for the LSKO or LGKO mice that were significantly different from the values for the control (*Shp2*$^{flox/flox}$ or *Gab1*$^{flox/flox}$) mice by a two-tailed unpaired *t* test are indicated as follows: *, $P < 0.05$; **, $P < 0.01$; ***, $P < 0.001$. Values are expressed as means ± standard errors of the means (SEMs) (error bars) ($n = 3$ to 7). (B) Representative samples of BrdU immunolabeling (green) were taken at 40, 44, and 68 h after PH. DAPI-stained nuclei are shown in red. Magnification, ×100. (C) Recuperation of the liver mass after PH. Liver weight per body weight was measured at 24, 48, and 72 h after surgery. Values are expressed as means ± SEMs (error bars) ($n = 3$ to 7). (D) Immunoblot analysis of cyclins A, B1, E, and D (with Erk2 as a loading control) was performed with liver lysates collected at the indicated time points after PH. Signals were quantified using ImageQuant software, with the strongest signal set at the value of 1.

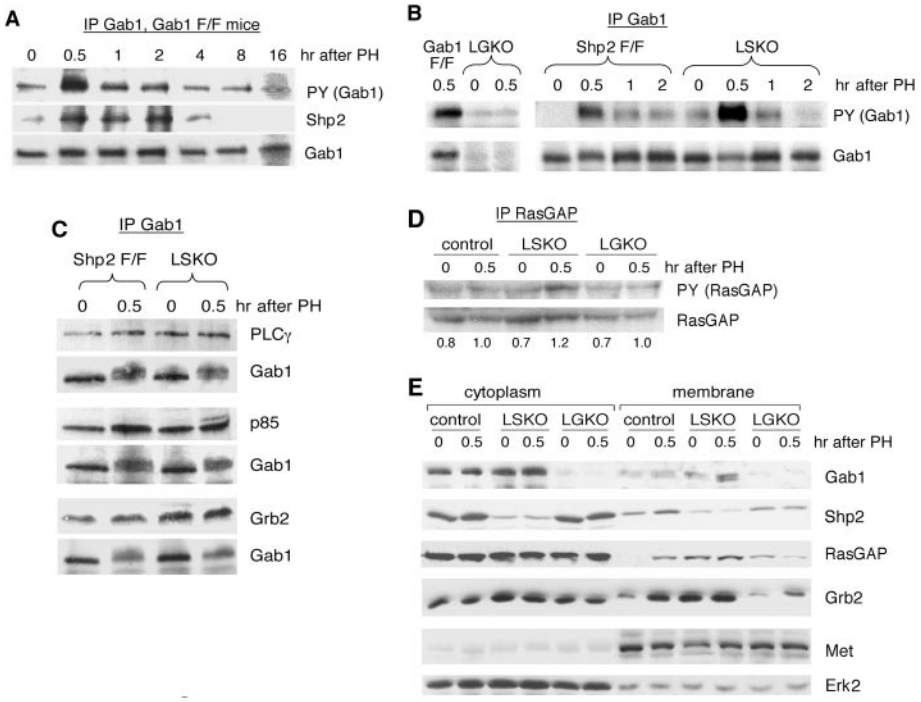

FIG. 3. Association of Gab1 and Shp2 at the plasma membrane after PH. (A) Control mice (*Gab1*$^{flox/flox}$ [Gab1 F/F]) were subjected to partial hepatectomy, and remnant livers were harvested at the indicated time points after surgery. Liver extracts were immunoprecipitated with an anti-Gab1 antibody (IP Gab1) and immunoblotted with antibodies against phosphotyrosine (PY), Gab1, or Shp2. (B) Liver extracts from *Gab1*$^{flox/flox}$ (Gab1 F/F) and LGKO mice and *Shp2*$^{flox/flox}$ (Shp2 F/F) and LSKO mice were immunoprecipitated with the Gab1 antibody and immunoblotted with antibodies to PY or Gab1. (C) Liver extracts were immunoprecipitated with the Gab1 antibody and immunoblotted with antibodies to the p85 subunit of PI3K, Grb2, PLC-γ, or Gab1. (D). RasGAP was precipitated with its specific antibody, and the immunoprecipitates were immunoblotted with antibodies to PY or RasGAP. Signals were quantified using ImageQuant software, with the strongest signal of controls set at the value of 1. (E) Cytoplasmic and plasma membrane-enriched fractions were isolated from livers collected at 0 and 0.5 h after PH. The lysates were subjected to immunoblotting with antibodies against Gab1, Shp2, RasGAP, and Grb2, with Met and Erk2 used as loading controls.

lysates were prepared at different time points following PH, Gab1 was precipitated with a specific antibody, and the resulting immunoprecipitates were immunoblotted with antibodies against PY, Shp2, or Gab1. As shown in Fig. 3A, Gab1 was highly phosphorylated on tyrosine 30 min after surgery, and high levels of Gab1 phosphorylation were sustained for 2 h. Notably, Shp2 tyrosine phosphatase was coimmunoprecipitated with Gab1 at these time points (Fig. 3A). Thus, partial hepatectomy triggered a rapid and transient phosphorylation of Gab1 on tyrosine, which induced formation of a signaling complex consisting of Gab1/Shp2, as well as other proteins. We then assessed Gab1 phosphorylation in liver lysates of LSKO mice and found that the tyrosine phosphorylation level of Gab1 was even higher in Shp2-deficient liver lysates than in control liver lysates 30 min after surgery (Fig. 3B). This observation strongly suggests that tyrosine phosphorylation of Gab1 itself is not sufficient but rather the important signaling event for promotion of hepatocyte proliferation is the assembly of a Gab1/Shp2 signalosome in the initial stage of liver regeneration. The association of p85, PLC-γ, and Grb2 with Gab1 observed in both LSKO and control samples (Fig. 3C) also suggests an indispensable role of the Gab1/Shp2 association in the proliferative response.

A number of putative Shp2 substrates have been proposed in the literature, including SHPS-1/SIRPα, PAG/Cbp, RasGAP and RasGAP binding sites on receptor tyrosine kinases (11, 23, 32, 55). Increased tyrosine phosphorylation levels of RasGAP was detected in LSKO lysates (Fig. 3D), supporting the theory that the Shp2 action may involve the modulation of RasGAP activity (31). However, we did not detect increased phosphorylation levels of SHPS-1/SIRPα or PAG/Cbp in liver lysates of the mutants (data not shown). Both Gab1 and Shp2 were mostly detected in the cytoplasmic fraction before surgery, but portions of the two proteins were recruited to the plasma membrane after PH (Fig. 3E). In LGKO liver, Shp2 content in the plasma membrane fraction was not increased after PH, suggesting a requirement for Gab1 in Shp2 relocation to the membrane. A recent report suggests that Gab1 is required for membrane relocation of RasGAP and that Shp2, by docking on Gab1, acts to regulate the association of Gab1/RasGAP, thereby promoting Ras activation (31). Consistently, we observed that Gab1 was required for RasGAP recruitment to the plasma membrane, and deletion of Shp2 resulted in increased amounts of RasGAP detected in the membrane fraction (Fig. 3E).

Both Shp2 and Gab1 are required for Erk activation by PH-initiated mitogenic signals. Activation of Erk1/2 enzymes is required to promote hepatocyte proliferation during liver regeneration stimulated by HGF, EGF, and IL-6 (6, 19, 24, 46). A peak level of p-Erk1/2 was detected in liver lysates from control mice at 30 min and progressively decreased during the subsequent 4 h after surgery (Fig. 4A). In contrast, p-Erk1/2

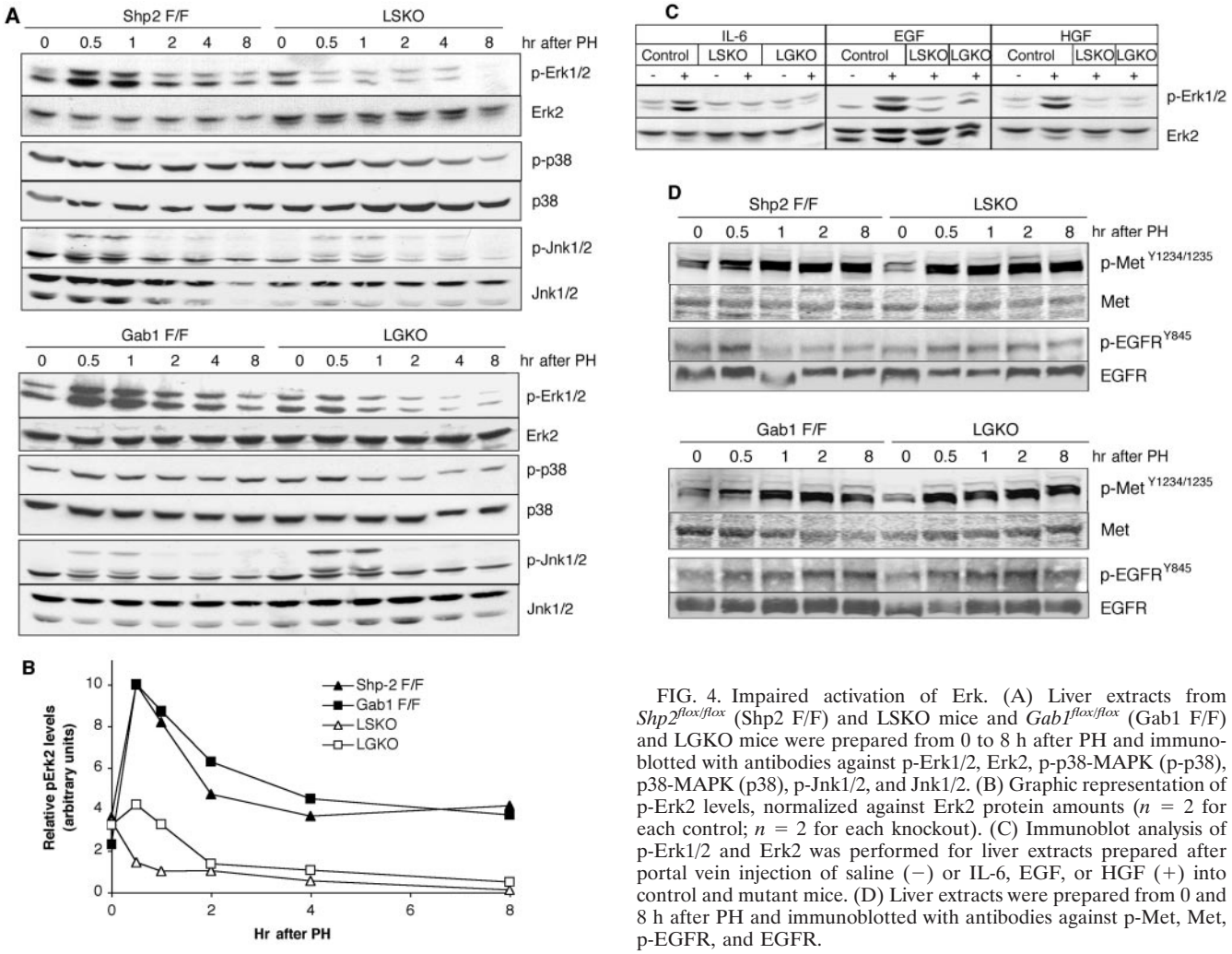

FIG. 4. Impaired activation of Erk. (A) Liver extracts from *Shp2*$^{flox/flox}$ (Shp2 F/F) and LSKO mice and *Gab1*$^{flox/flox}$ (Gab1 F/F) and LGKO mice were prepared from 0 to 8 h after PH and immunoblotted with antibodies against p-Erk1/2, Erk2, p-p38-MAPK (p-p38), p38-MAPK (p38), p-Jnk1/2, and Jnk1/2. (B) Graphic representation of p-Erk2 levels, normalized against Erk2 protein amounts ($n = 2$ for each control; $n = 2$ for each knockout). (C) Immunoblot analysis of p-Erk1/2 and Erk2 was performed for liver extracts prepared after portal vein injection of saline (−) or IL-6, EGF, or HGF (+) into control and mutant mice. (D) Liver extracts were prepared from 0 and 8 h after PH and immunoblotted with antibodies against p-Met, Met, p-EGFR, and EGFR.

induction was blunted in liver lysates of either LSKO or LGKO mice posthepatectomy (Fig. 4A and B), indicating a requirement of both Gab1 and Shp2 for promotion of the Erk pathway.

The results described above strongly suggest a cooperative role of Gab1 and Shp2 in mediating hepatic mitogenic signals through stimulation of the Erk pathway. To directly examine the requirement of Gab1 and Shp2 for Erk activation by growth factors/cytokines, we injected HGF, EGF, or IL-6 into the portal vein and prepared liver lysates 5 min after stimulation. Immunoblot analysis demonstrated a potent induction of Erk1/2 activation by all three factors in control mice, but this induction was blunted in livers from LSKO or LGKO mice (Fig. 4C). Analysis of other members of the mitogen-activated protein kinase (MAPK) family revealed that Gab1 and Shp2 deletions also decreased p38 activation. Although PH-induced p38 activation was not as profound as Erk activation in control animals, both knockout samples displayed reduced levels of phospho-p38 (Fig. 4A). On the other hand, induction of phospho-Jnk1/2 was similar or slightly increased in both knockout mice compared to the controls (Fig. 4A). We also examined the expression and tyrosine phosphorylation levels of c-Met and EGFR at the initial stage of liver regeneration and did not detect a significant change in either LSKO or LGKO liver lysates compared to the controls (Fig. 4D), suggesting that Shp2 acts mainly in downstream signaling events of the receptors.

Deletion of Shp2 or Gab1 down-regulates PH-induced expression of immediate-early genes. Activation of the Erk pathway leads to expression of immediate-early genes required for initiation of hepatocyte proliferation during liver regeneration (6, 19, 24, 46). Immunoblot analysis of liver lysates using a pan-Fos antibody demonstrated a strong induction of pan-Fos protein expression in control animals posthepatectomy (Fig. 5A), whereas the pan-Fos signal was barely detectable in lysates from either knockout. To broadly evaluate the immediate-early gene expression status, we performed real-time RT-PCR analysis and assessed the levels of transcripts for c-*Fos*, c-*Jun*, c-*Myc*, and *C/EBP*β, at 1, 4, and 8 h posthepatectomy (Fig. 5B). In control animals, peak levels of c-*Fos* and c-*Jun* expression were detected 1 h after surgery, and their expression declined rapidly to basal levels, as evaluated at 4 and 8 h posthepatectomy. However, PH-induced c-*Fos* and c-*Jun* expression was dramatically reduced in the livers of LSKO and

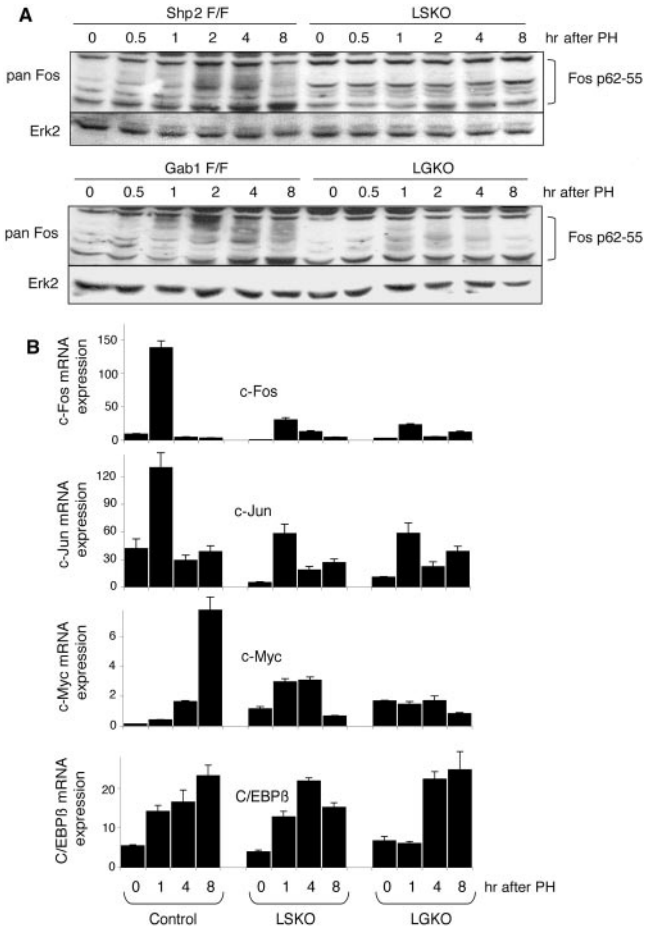

FIG. 5. Impaired expression of immediate-early genes. (A) Liver extracts from *Shp2*$^{flox/flox}$ (Shp2 F/F) and LSKO mice and *Gab1*$^{flox/flox}$ (Gab1 F/F) and LGKO mice were prepared and immunoblotted with an antibody to pan-Fos. The migration positions of the different family members range from 55 to 62 kDa. (B) Expression levels of c-*Fos*, c-*Jun*, c-*Myc*, and *C/EBP*β mRNAs. Total RNAs were isolated from hepatectomized livers and assessed by real-time RT-PCR. Values are expressed as means ± standard errors of the means (SEMs) (error bars). The results shown are from three different mice per time point and genotype.

LGKO mice (Fig. 5B). Lower levels of *c-Myc* mRNA were also observed in liver lysates of LSKO and LGKO mice than in the liver lysates of control mice. Although impaired phosphorylation of Erk1/2 has been correlated with a reduced *C/EBP*β expression in hepatocytes during liver regeneration (24), we detected normal *C/EBP*β mRNA levels in liver lysates prepared from both LSKO and LGKO mice (Fig. 5B).

Gab1 and Shp2 negatively regulate Stat3 activation in liver regeneration. Activation of Stat3 has been shown to contribute to hepatocyte proliferation and liver regeneration posthepatectomy (7, 25). To determine the status of Stat3 activation, we first evaluated induction of *Stat3* mRNA expression using real-time RT-PCR. A similar profile of *Stat3* gene expression was detected in liver lysates of control, LSKO, and LGKO mice when analyzed at 0, 1, 4 and 8 h after surgery (Fig. 6A). We then evaluated the phosphorylation levels of Stat3 on Tyr^{705} by immunoblot analysis with the site-specific antibody of liver lysates. Phosphorylation of Stat3 on Tyr^{705} was detectable in control mice 30 min after surgery and rose slowly until 8 h. Surprisingly, higher levels of p-Stat3(Tyr^{705}) were detected in the two mutant liver lysates than in the control liver lysates (Fig. 6B and C). Tyrosine phosphorylation of Stat1 and Stat5 could not be detected in the liver lysates of control, LSKO, or LGKO mice posthepatectomy (data not shown). Although there was a modest increase in the *Stat3* mRNA levels at the initial stages of liver regeneration (Fig. 6A), we did not detect a significant change in the amount of Stat3 protein in the liver lysates analyzed at the same time points (Fig. 6B).

We performed gel mobility shift assay to assess the DNA binding activity of Stat3 as a transcription factor. Nuclear extracts were prepared from the livers of control and mutant mice 4 and 5 h after surgery. Consistent with the data shown in Fig. 6B, the gel shift assay showed a significantly enhanced Stat3 activation in the livers of both LSKO and LGKO mice compared to the livers of control mice (Fig. 6D), suggesting that the Gab1/Shp2 pathway has a negative impact on Stat3 activation during liver regeneration. Alternatively, the enhanced Stat3 activation may be a compensation mechanism in Gab1- or Shp2-deficient livers.

Growth factor/cytokine levels are not reduced in LSKO and LGKO mice posthepatectomy. We determined whether the impaired Erk activation and hepatocyte proliferation are due to decreased production of growth factors following PH by real-time RT-PCR analysis. As shown in Fig. 7A, production of *HGF* mRNA was normal in the livers of both LSKO and LGKO animals. The synthesis of *EGF* mRNA in regenerating liver was much lower than that of *HGF* transcript in control and mutant animals (Fig. 7A). Normal expression of *HGF* mRNA suggests that deletion of Shp2 or Gab1 causes uncoupling of intracellular signaling cascades rather than defective production of growth factors, resulting in down-regulation of the Erk pathway. Consistently, similar levels of p-Met and p-EGFR were detected in LSKO and LGKO liver lysates compared to the control liver lysates (Fig. 4D). *IL-6* mRNA levels were elevated by 5.7-fold in LSKO livers compared to control livers at 4 h after surgery, whereas LGKO liver showed a modest increase in *IL-6* gene expression. Production of *TNF*-α mRNA in the liver in control and LSKO mice was comparable with modestly reduced levels seen in LGKO mice (Fig. 7A).

Enhanced IL-6/Stat3 and Akt pathways are associated with decreased liver damage. During liver regeneration, the serum IL-6 level rises rapidly, due to enhanced production by Kupffer cells (51, 52). We measured by enzyme-linked immunosorbent assay the serum IL-6 concentrations at several time points after surgery and detected an increase in IL-6 levels beginning 2 h after surgery in control animals (Fig. 7B). Notably, the IL-6 levels were dramatically elevated in LSKO mice at 2, 4, and 8 h, and a significant increase of serum IL-6 was also detected in LGKO mice 2 h posthepatectomy.

IL-6 signaling is implicated in hepatoprotection by reducing both apoptosis and necrosis in different conditions (47). Consistent with previous findings (24), serum levels of two liver enzymes released upon hepatic damage, aspartate aminotransferase and alanine aminotransferase, were increased in control animals after PH and peaked at 20 h. At that time point, the amount of AST was reduced by 42% in LSKO and by 53% in LGKO samples, compared to the controls. Similarly, serum

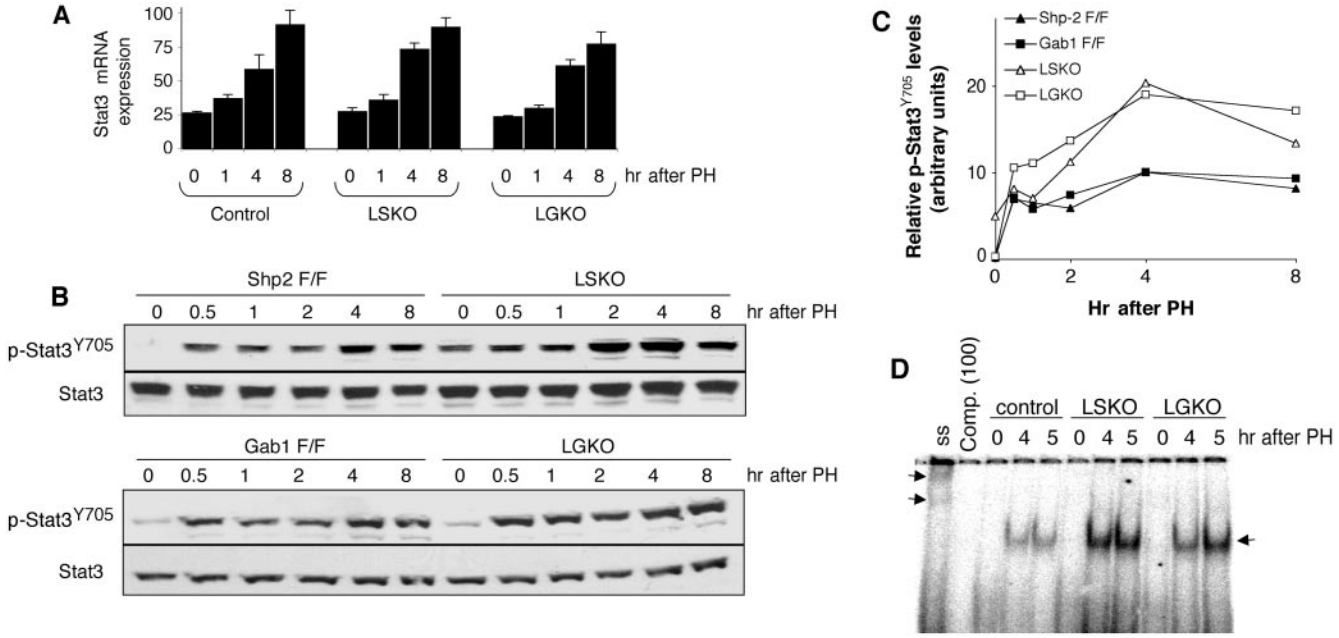

FIG. 6. Enhanced Stat3 activation. (A) *Stat3* mRNA levels from control (*Shp2*$^{flox/flox}$ or *Gab1*$^{flox/flox}$), LSKO, and LGKO mice. Real-time RT-PCR analysis was performed as described in the legend to Fig. 5B. (B) Induction of p-Tyr^{705}Stat3 was measured at 0 to 8 h after PH by immunoblotting of liver extracts. The liver extracts were from *Shp2*$^{flox/flox}$ (Shp2 F/F) and LSKO mice and *Gab1*$^{flox/flox}$ (Gab1 F/F) and LGKO mice. (C) Graphic representation of p-Tyr^{705}Stat3 levels normalized against Stat3 protein amounts ($n = 2$ for each control; $n = 2$ for each knockout). (D) Stat3 DNA binding activity was assessed by gel mobility shift assay with nuclear extracts. The leftmost lane shows a supershift (ss) when Stat3 antibody was added to control extract prepared at 5 h. The next lane shows a competition (Comp.) assay in which 50 ng of cold probe was added to the control extract at 5 h.

ALT levels were decreased by 57% and 52% in LSKO and LGKO mice, respectively (Fig. 7C). The reduced hepatocellular damage seen in both knockout animals was accompanied by a significantly elevated expression of a hepatic acute-phase gene encoding hemopexin in both LSKO and LGKO livers. However, the expression of the antiapoptotic *Bcl-xl* gene was normal or modestly reduced in both knockout mice (Fig. 7A).

Higher levels of phospho-Akt were detected in both LSKO and LGKO mice than in control mice (Fig. 7D), which may also mediate hepatoprotective effects, as suggested by a previous study (18). Consistently, the levels of p-MDM2 (Ser166), p-Bad (Ser136), and p-GSK3, substrates of Akt, were relatively increased in the mutants compared to the controls (Fig. 7D).

DISCUSSION

Remarkably, PH-triggered liver regeneration is not dependent on a small population of stem cells in the liver (30, 49), but rather on quiescent and differentiated hepatocytes which can rapidly acquire proliferative competence and respond to elevated growth factor signals for DNA synthesis and proliferation. How the intracellular signals are transduced in hepatocytes to trigger such a proliferative response is not fully understood. By creating liver-specific gene knockout animals, we have identified critical roles of both the Gab1 adaptor protein and Shp2 tyrosine phosphatase in mitogenic signaling post-hepatectomy. We show that Gab1 and Shp2 associate to form a complex in hepatocytes rapidly and transiently in the initial stage of liver regeneration, which is evidently required for stimulation of the Erk pathway, expression of immediate-early responsive genes, and DNA synthesis. Thus, this study reveals a missing link in the intracellular signaling cascade mediating proliferation of quiescent hepatocytes. Prior studies by several groups demonstrated a physical interaction of Gab1 and Shp2 in a variety of cell types in vitro (13, 17, 23, 41, 45). However, in those experiments, the Gab1/Shp2 complex was detected in cells treated with saturating amounts of a cytokine/growth factor. To our knowledge, this study presents the first physiological evidence that Gab1 is phosphorylated on tyrosine and associates with Shp2 in response to endogenous growth factor signals in regenerating livers in mammals.

Gab1 tyrosine phosphorylation and binding to Shp2 occurred 30 min after surgery, suggesting that these proteins act in the induction phase of liver regeneration. Interestingly, in hepatectomized LSKO livers, the Gab1 phosphorylation level detected 30 min posthepatectomy was even higher than that seen in the control. This observation suggests a role for Shp2 in dephosphorylating Gab1, supporting the previous in vitro biochemical data (8, 31, 33, 54). A similar dephosphorylation effect was observed for corkscrew (the Shp2 homologue) on Dos, daughter of sevenless (the Gab1 homologue) in *Drosophila melanogaster* (15). We further demonstrate that Shp2 may modulate the interaction of Gab1 with RasGAP, thereby promoting the Ras-Erk pathway. However, more work is needed to elucidate the molecular mechanism for Shp2/Gab1 action in mitogenic signaling of hepatocytes, and it is likely that more than one substrate is involved in mediating the Shp2 function.

It is noteworthy that hepatocyte proliferation rates were similarly decreased in regenerating livers of LSKO and LGKO mice,

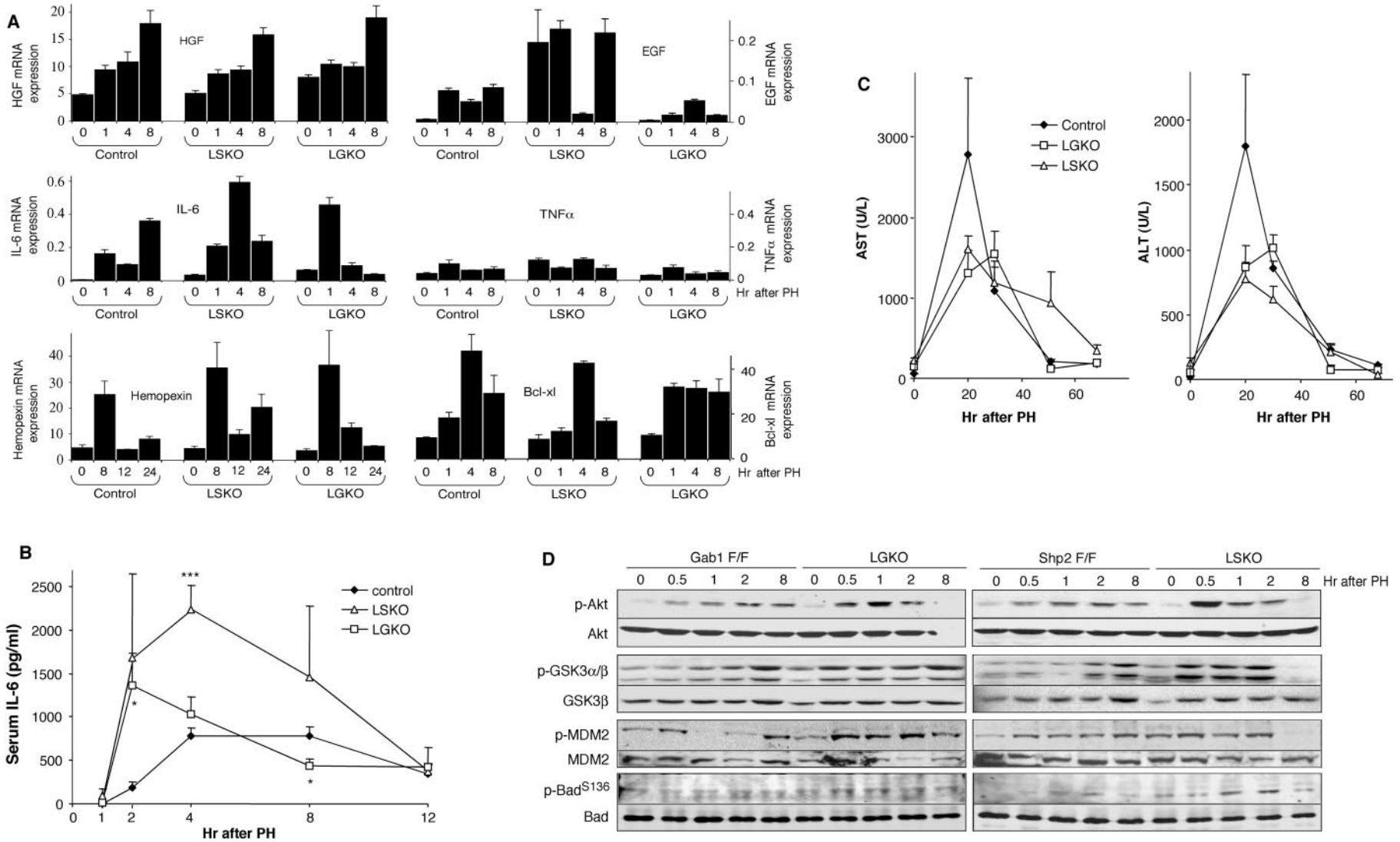

FIG. 7. Enhanced IL-6 production and p-Akt levels. (A) Levels of *HGF*, *EGF*, *IL-6*, *TNF*-α, *Stat3*, *hemopexin*, and *Bcl-xl* mRNAs were assessed by real-time RT-PCR. Values are expressed as means ± standard errors of the means (SEMs) (error bars). The results are representative of three mice. (B) Circulating blood levels of IL-6 were quantified at the indicated time points posthepatectomy. Values for the LSKO or LGKO mice that were significantly different from the values for the control ($Shp2^{flox/flox}$ or $Gab1^{flox/flox}$) mice by a two-tailed unpaired *t* test are indicated as follows: *, $P < 0.05$; ***, $P < 0.001$. Values are expressed as means ± SEMs (error bars) ($n = 3$ to 5). (C) Circulating blood levels of AST and ALT (in units per liter) were quantified at different time points after surgery. Values are expressed as means ± SEMs (error bars) ($n = 3$ or 4). (D) p-Akt, p-GSK3, p-MDM2, and p-Bad levels were evaluated at 0 to 8 h after PH by immunoblotting of liver extracts from $Gab1^{flox/flox}$ (Gab1 F/F) and LGKO mice and $Shp2^{flox/flox}$ (Shp2 F/F) and LSKO mice. Akt, GSK3, MDM2, and Bad were used as loading controls.

with no changes seen in the kinetics of DNA synthesis posthepatectomy. Expression levels of growth factors such as HGF in regenerating livers were not significantly changed in either mutant liver after surgery, nor was there a significant change in the expression and phosphorylation levels of HGF and EGF receptors. Thus, deletion of Shp2 or Gab1 in hepatocytes did not affect the expression of growth factors and activation of their receptors but rather suppressed their downstream signaling cascades. Impaired cell cycle progression seen in LSKO and LGKO livers is likely caused by a deficit in Erk activation posthepatectomy (Fig. 4A). That Gab1 and Shp2 are required for mitogenic stimulation of Erk activity was further evidenced by the blunted Erk1/2 activation in the liver in vivo following intraperitoneal injection of HGF, EGF, or IL-6 into LSKO and LGKO mice. Yet, the observation that the LGKO mouse phenocopies LSKO animal in liver regeneration is unanticipated, as it has been well documented that Gab1 can bind a number of other signaling proteins, such as Shc, CrkL, PI3K, PLC-γ, and Grb2. Shp2 can also interact through its two SH2 domains with several cytoplasmic signaling proteins that are tyrosine phosphorylated. These multiple protein-protein interactions constitute a network that allows intracellular signals flow through interconnected parallel routes. This model predicts that loss of Gab1 or Shp2 could be compensated by their functional partners in the signaling network, likely leading to different phenotypes of LGKO and LSKO mice. However, the similar defects in liver regeneration seen in these two mutants argue that despite the multiple interactions likely engaged by both proteins, the Gab1/Shp2 link is indispensable for mitogenic signaling in hepatocytes.

Reduced Erk signals are connected with impaired cell cycle progression in mutant liver cells, which was evidenced by decreased expression of cyclins A, E, and B1. However, cyclin D1 expression was not significantly changed in LSKO and LGKO livers following PH. Notably, a similar expression profile of cell cycle regulatory proteins was observed in *C/EBP*$\beta^{-/-}$ and *IGFBP-1*$^{-/-}$ mice (12, 24). Deletion of Gab1 or Shp2 might not affect the priming induced by TNF-α but rather suppress mitogenic signals elicited by growth factors, such as HGF and EGF. Indeed, a subset of immediate-early genes, including c-*Fos*, c-*Jun*, and c-*Myc*, exhibited impaired activation in hepatectomized LSKO and LGKO mice (Fig. 5B).

Enhanced IL-6/Stat3 signaling was observed in both LSKO and LGKO mice. Previous experiments demonstrated a significant contribution of the IL-6/Stat3 pathway to mitogenic signaling required for liver regeneration (7, 25, 28). This may explain why the hepatocyte proliferation capacity in regenerating livers of LSKO and LGKO mice was significantly impaired but not completely blocked. Compared to control animals, LSKO mice showed dramatically increased serum IL-6 levels as did LGKO mice to a lesser extent, following PH. Increased IL-6 secretion was also reported in liver-specific c-Met knockout mice posthepatectomy, possibly as a compensatory mechanism for impaired liver regeneration (6). IL-6 is secreted via a paracrine mechanism by Kupffer cells stimulated by TNF-α or other factors (1). The more profound increase of IL-6 in LSKO mice compared to LGKO mice may also be due to hepatic inflammation seen in some LSKO livers. Indeed, we detected infiltration of inflammatory cells in some LSKO livers (our unpublished results). The IL-6/Stat3 pathway is also implicated in hepatoprotection by antagonizing necrosis and apoptosis following PH or in response to other insults (47). Consistently, we found that the expression of an acute-phase response gene encoding hemopexin was significantly increased in LSKO and LGKO animals (Fig. 7A), consistent with a previous observation that Shp2 is not required for the induction of acute-phase plasma protein genes in hepatic cells (21). These results suggest that improved hepatoprotection is related to an enhanced acute-phase response. Also, increased activation of Akt kinase and its downstream targets, such as Bad and MDM2 involved in cell survival, in the regenerating livers of LSKO and LGKO mice may contribute to an improved hepatoprotective effect as well (18).

In contrast to the similar proliferative signaling defects, we have observed opposite phenotypes in LSKO and LGKO mice with regard to insulin signaling in the liver. In another study, we demonstrated that LGKO mice displayed enhanced hepatic insulin sensitivity and improved glucose tolerance and that Gab1 suppressed insulin-elicited signal flow through IRS1 and IRS2 proteins (2). However, LSKO mice exhibited mild insulin resistance in the liver (our unpublished data), suggesting that Shp2 is positively required for insulin action in hepatocytes. Evidently, different mechanisms are involved in mitogenic and metabolic signaling in hepatocytes in vivo. As shown in this study, a Gab1/Shp2 complex is rapidly assembled in regenerating livers to mediate the proliferative signals. However, Gab1 is poorly tyrosine phosphorylated, and it does not associate with Shp2 in insulin-stimulated livers (2). Apparently, Gab1 and Shp2 have distinct functions in mediating hepatic response to insulin stimulation by working with different partners. Therefore, we propose that specific and efficient pharmaceutical intervention of malignant or insulin-resistant processes in human subjects may require disruption of a specific signaling complex, rather than inhibition of a specific enzyme that may participate in multiple pathways.

ACKNOWLEDGMENTS

We thank W. Jiang and A. Veillette for antibodies and A. Guio-Carrion for running the real-time RT-PCR.

This work was supported by grants from NIH (CA78606 and GM53660) to G.-S.F.

REFERENCES

1. **Aldeguer, X., F. Debonera, A. Shaked, A. M. Krasinkas, A. E. Gelman, X. Que, G. A. Zamir, S. Hiroyasu, K. K. Kovalovich, R. Taub, and K. M. Olthoff.** 2002. Interleukin-6 from intrahepatic cells of bone marrow origin is required for normal murine liver regeneration. Hepatology **35:**40–48.
2. **Bard-Chapeau, E. A., A. L. Hevener, S. Long, E. E. Zhang, J. M. Olefsky, and G. S. Feng.** 2005. Deletion of Gab1 in the liver leads to enhanced glucose tolerance and improved hepatic insulin action. Nat. Med. **11:**567–571.
3. **Bardin, A. J., and A. Amon.** 2001. Men and sin: what's the difference? Nat. Rev. Mol. Cell Biol. **2:**815–826.
4. **Bladt, F., D. Riethmacher, S. Isenmann, A. Aguzzi, and C. Birchmeier.** 1995. Essential role for the c-met receptor in the migration of myogenic precursor cells into the limb bud. Nature **376:**768–771.
5. **Blindenbacher, A., X. Wang, I. Langer, R. Savino, L. Terracciano, and M. H. Heim.** 2003. Interleukin 6 is important for survival after partial hepatectomy in mice. Hepatology **38:**674–682.
6. **Borowiak, M., A. N. Garratt, T. Wustefeld, M. Strehle, C. Trautwein, and C. Birchmeier.** 2004. Met provides essential signals for liver regeneration. Proc. Natl. Acad. Sci. USA **101:**10608–10613.
7. **Cressman, D. E., L. E. Greenbaum, R. A. DeAngelis, G. Ciliberto, E. E. Furth, V. Poli, and R. Taub.** 1996. Liver failure and defective hepatocyte regeneration in interleukin-6-deficient mice. Science **274:**1379–1383.
8. **Cunnick, J. M., L. Mei, C. A. Doupnik, and J. Wu.** 2001. Phosphotyrosines 627 and 659 of Gab1 constitute a bisphosphoryl tyrosine-based activation motif (BTAM) conferring binding and activation of SHP2. J. Biol. Chem. **276:**24380–24387.

9. **Fausto, N.** 2000. Liver regeneration. J. Hepatol. **32:**19–31.
10. **Fausto, N., A. D. Laird, and E. M. Webber.** 1995. Liver regeneration. 2. Role of growth factors and cytokines in hepatic regeneration. FASEB J. **9:**1527–1536.
11. **Feng, G. S.** 1999. Shp-2 tyrosine phosphatase: signaling one cell or many. Exp. Cell Res. **253:**47–54.
12. **Greenbaum, L. E., W. Li, D. E. Cressman, Y. Peng, G. Ciliberto, V. Poli, and R. Taub.** 1998. CCAAT enhancer-binding protein beta is required for normal hepatocyte proliferation in mice after partial hepatectomy. J. Clin. Investig. **102:**996–1007.
13. **Gu, H., and B. G. Neel.** 2003. The "Gab" in signal transduction. Trends Cell Biol. **13:**122–130.
14. **Haber, B. A., K. L. Mohn, R. H. Diamond, and R. Taub.** 1993. Induction patterns of 70 genes during nine days after hepatectomy define the temporal course of liver regeneration. J. Clin. Investig. **91:**1319–1326.
15. **Herbst, R., P. M. Carroll, J. D. Allard, J. Schilling, T. Raabe, and M. A. Simon.** 1996. Daughter of sevenless is a substrate of the phosphotyrosine phosphatase Corkscrew and functions during sevenless signaling. Cell **85:**899–909.
16. **Higgins, G. M., and R. M. Anderson.** 1931. Experimental pathology of the liver. I. Restoration of the liver of the white rat following partial surgical removal. Arch. Pathol. **12:**186–202.
17. **Holgado-Madruga, M., D. R. Emlet, D. K. Moscatello, A. K. Godwin, and A. J. Wong.** 1996. A Grb2-associated docking protein in EGF- and insulin-receptor signalling. Nature **379:**560–564.
18. **Hong, F., V. A. Nguyen, X. Shen, G. Kunos, and B. Gao.** 2000. Rapid activation of protein kinase B/Akt has a key role in antiapoptotic signaling during liver regeneration. Biochem. Biophys. Res. Commun. **279:**974–979.
19. **Huh, C. G., V. M. Factor, A. Sanchez, K. Uchida, E. A. Conner, and S. S. Thorgeirsson.** 2004. Hepatocyte growth factor/c-met signaling pathway is required for efficient liver regeneration and repair. Proc. Natl. Acad. Sci. USA **101:**4477–4482.
20. **Itoh, M., Y. Yoshida, K. Nishida, M. Narimatsu, M. Hibi, and T. Hirano.** 2000. Role of Gab1 in heart, placenta, and skin development and growth factor- and cytokine-induced extracellular signal-regulated kinase mitogen-activated protein kinase activation. Mol. Cell. Biol. **20:**3695–3704.
21. **Kim, H., T. S. Hawley, R. G. Hawley, and H. Baumann.** 1998. Protein tyrosine phosphatase 2 (SHP-2) moderates signaling by gp130 but is not required for the induction of acute-phase plasma protein genes in hepatic cells. Mol. Cell. Biol. **18:**1525–1533.
22. **Klein, C., T. Wustefeld, U. Assmus, T. Roskams, S. Rose-John, M. Muller, M. P. Manns, M. Ernst, and C. Trautwein.** 2005. The IL-6-gp130-STAT3 pathway in hepatocytes triggers liver protection in T cell-mediated liver injury. J. Clin. Investig. **115:**860–869.
23. **Lai, L. A., C. Zhao, E. E. Zhang, and G. S. Feng.** 2003. The Shp-2 tyrosine phosphatase, p. 275–299. *In* J. Arino and D. Alexander (ed.), Protein phosphatases, vol. 5. Springer-Verlag, Berlin, Germany.
24. **Leu, J. I., M. A. Crissey, L. E. Craig, and R. Taub.** 2003. Impaired hepatocyte DNA synthetic response posthepatectomy in insulin-like growth factor binding protein 1-deficient mice with defects in C/EBPβ and mitogen-activated protein kinase/extracellular signal-regulated kinase regulation. Mol. Cell. Biol. **23:**1251–1259.
25. **Li, W., X. Liang, C. Kellendonk, V. Poli, and R. Taub.** 2002. STAT3 contributes to the mitogenic response of hepatocytes during liver regeneration. J. Biol. Chem. **277:**28411–28417.
26. **Liu, Y., and L. R. Rohrschneider.** 2002. The gift of Gab. FEBS Lett. **515:**1–7.
27. **Maina, F., F. Casagranda, E. Audero, A. Simeone, P. M. Comoglio, R. Klein, and C. Ponzetto.** 1996. Uncoupling of Grb2 from the Met receptor in vivo reveals complex roles in muscle development. Cell **87:**531–542.
28. **Maione, D., E. Di Carlo, W. Li, P. Musiani, A. Modesti, M. Peters, S. Rose-John, C. Della Rocca, M. Tripodi, D. Lazzaro, R. Taub, R. Savino, and G. Ciliberto.** 1998. Coexpression of IL-6 and soluble IL-6R causes nodular regenerative hyperplasia and adenomas of the liver. EMBO J. **17:**5588–5597.
29. **Michael, M. D., R. N. Kulkarni, C. Postic, S. F. Previs, G. I. Shulman, M. A. Magnuson, and C. R. Kahn.** 2000. Loss of insulin signaling in hepatocytes leads to severe insulin resistance and progressive hepatic dysfunction. Mol. Cell **6:**87–97.
30. **Michalopoulos, G. K., and M. C. DeFrances.** 1997. Liver regeneration. Science **276:**60–66.
31. **Montagner, A., A. Yart, M. Dance, B. Perret, J. P. Salles, and P. Raynal.** 2005. A novel role for Gab1 and SHP2 in epidermal growth factor-induced Ras activation. J. Biol. Chem. **280:**5350–5360.
32. **Neel, B. G., H. Gu, and L. Pao.** 2003. The 'Shp'ing news: SH2 domain-containing tyrosine phosphatases in cell signaling. Trends Biochem. Sci. **28:**284–293.
33. **Nishida, K., Y. Yoshida, M. Itoh, T. Fukada, T. Ohtani, T. Shirogane, T. Atsumi, M. Takahashi-Tezuka, K. Ishihara, M. Hibi, and T. Hirano.** 1999. Gab-family adapter proteins act downstream of cytokine and growth factor receptors and T- and B-cell antigen receptors. Blood **93:**1809–1816.
34. **Postic, C., M. Shiota, K. D. Niswender, T. L. Jetton, Y. Chen, J. M. Moates, K. D. Shelton, J. Lindner, A. D. Cherrington, and M. A. Magnuson.** 1999. Dual roles for glucokinase in glucose homeostasis as determined by liver and pancreatic beta cell-specific gene knock-outs using Cre recombinase. J. Biol. Chem. **274:**305–315.
35. **Qu, C. K.** 2002. Role of the SHP-2 tyrosine phosphatase in cytokine-induced signaling and cellular response. Biochim. Biophys. Acta **1592:**297–301.
36. **Qu, C. K., W. M. Yu, B. Azzarelli, S. Cooper, H. E. Broxmeyer, and G. S. Feng.** 1998. Biased suppression of hematopoiesis and multiple developmental defects in chimeric mice containing Shp-2 mutant cells. Mol. Cell. Biol. **18:**6075–6082.
37. **Sachs, M., H. Brohmann, D. Zechner, T. Muller, J. Hulsken, I. Walther, U. Schaeper, C. Birchmeier, and W. Birchmeier.** 2000. Essential role of Gab1 for signaling by the c-Met receptor in vivo. J. Cell Biol. **150:**1375–1384.
38. **Saxton, T. M., M. Henkemeyer, S. Gasca, R. Shen, D. J. Rossi, F. Shalaby, G. S. Feng, and T. Pawson.** 1997. Abnormal mesoderm patterning in mouse embryos mutant for the SH2 tyrosine phosphatase Shp-2. EMBO J. **16:**2352–2364.
39. **Saxton, T. M., and T. Pawson.** 1999. Morphogenetic movements at gastrulation require the SH2 tyrosine phosphatase Shp2. Proc. Natl. Acad. Sci. USA **96:**3790–3795.
40. **Schmidt, C., F. Bladt, S. Goedecke, V. Brinkmann, W. Zschiesche, M. Sharpe, E. Gherardi, and C. Birchmeier.** 1995. Scatter factor/hepatocyte growth factor is essential for liver development. Nature **373:**699–702.
41. **Shi, Z. Q., D. H. Yu, M. Park, M. Marshall, and G. S. Feng.** 2000. Molecular mechanism for the Shp-2 tyrosine phosphatase function in promoting growth factor stimulation of Erk activity. Mol. Cell. Biol. **20:**1526–1536.
42. **Strom, S. C., L. A. Pisarov, K. Dorko, M. T. Thompson, J. D. Schuetz, and E. G. Schuetz.** 1996. Use of human hepatocytes to study P450 gene induction. Methods Enzymol. **272:**388–401.
43. **Su, A. I., L. G. Guidotti, J. P. Pezacki, F. V. Chisari, and P. G. Schultz.** 2002. Gene expression during the priming phase of liver regeneration after partial hepatectomy in mice. Proc. Natl. Acad. Sci. USA **99:**11181–11186.
44. **Sun, Y., J. Yuan, H. Liu, Z. Shi, K. Baker, K. Vuori, J. Wu, and G. S. Feng.** 2004. Role of Gab1 in UV-induced c-Jun NH_2-terminal kinase activation and cell apoptosis. Mol. Cell. Biol. **24:**1531–1539.
45. **Takahashi-Tezuka, M., Y. Yoshida, T. Fukada, T. Ohtani, Y. Yamanaka, K. Nishida, K. Nakajima, M. Hibi, and T. Hirano.** 1998. Gab1 acts as an adapter molecule linking the cytokine receptor gp130 to ERK mitogen-activated protein kinase. Mol. Cell. Biol. **18:**4109–4117.
46. **Talarmin, H., C. Rescan, S. Cariou, D. Glaise, G. Zanninelli, M. Bilodeau, P. Loyer, C. Guguen-Guillouzo, and G. Baffet.** 1999. The mitogen-activated protein kinase kinase/extracellular signal-regulated kinase cascade activation is a key signalling pathway involved in the regulation of G_1 phase progression in proliferating hepatocytes. Mol. Cell. Biol. **19:**6003–6011.
47. **Taub, R.** 2003. Hepatoprotection via the IL-6/Stat3 pathway. J. Clin. Investig. **112:**978–980.
48. **Taub, R.** 2004. Liver regeneration: from myth to mechanism. Nat. Rev. Mol. Cell Biol. **5:**836–847.
49. **Thorgeirsson, S. S.** 1996. Hepatic stem cells in liver regeneration. FASEB J. **10:**1249–1256.
50. **Uehara, Y., O. Minowa, C. Mori, K. Shiota, J. Kuno, T. Noda, and N. Kitamura.** 1995. Placental defect and embryonic lethality in mice lacking hepatocyte growth factor/scatter factor. Nature **373:**702–705.
51. **Yamada, Y., I. Kirillova, J. J. Peschon, and N. Fausto.** 1997. Initiation of liver growth by tumor necrosis factor: deficient liver regeneration in mice lacking type I tumor necrosis factor receptor. Proc. Natl. Acad. Sci. USA **94:**1441–1446.
52. **Yamada, Y., E. M. Webber, I. Kirillova, J. J. Peschon, and N. Fausto.** 1998. Analysis of liver regeneration in mice lacking type 1 or type 2 tumor necrosis factor receptor: requirement for type 1 but not type 2 receptor. Hepatology **28:**959–970.
53. **Zhang, E. E., E. Chapeau, K. Hagihara, and G. S. Feng.** 2004. Neuronal Shp2 tyrosine phosphatase controls energy balance and metabolism. Proc. Natl. Acad. Sci. USA **101:**16064–16069.
54. **Zhang, S. Q., W. G. Tsiaras, T. Araki, G. Wen, L. Minichiello, R. Klein, and B. G. Neel.** 2002. Receptor-specific regulation of phosphatidylinositol 3′-kinase activation by the protein tyrosine phosphatase Shp2. Mol. Cell. Biol. **22:**4062–4072.
55. **Zhang, S. Q., W. Yang, M. I. Kontaridis, T. G. Bivona, G. Wen, T. Araki, J. Luo, J. A. Thompson, B. L. Schraven, M. R. Philips, and B. G. Neel.** 2004. Shp2 regulates SRC family kinase activity and Ras/Erk activation by controlling Csk recruitment. Mol. Cell **13:**341–355.
56. **Zimmers, T. A., R. H. Pierce, I. H. McKillop, and L. G. Koniaris.** 2003. Resolving the role of IL-6 in liver regeneration. Hepatology **38:**1590–1591.